Journal of Materials Chemistry B

Accepted Manuscript

ROYAL SOCIETY OF CHEMISTRY

www.rsc.org/materialsB

Journal Name

ARTICLE

Cell response on Biomimetic Scaffold of Silicon Nano- and Micro-Topography

Received 00th January 20xx,
Accepted 00th January 20xx

DOI: 10.1039/x0xx00000x

www.rsc.org/

Shih-Ping Yang[a], Hsiang-Sheng Wen[b], Tzer-Min Lee[c,d*] and Truan-Sheng Lui[a]

Silicon scaffolds were synthesized in a low-pressure furnace via vapor-liquid-solid (VLS) mechanism. Structural dimensions of silicon scaffolds were tunable in the synthesis to satisfy diverse requirements for cell culture applications. Cylindraceous SiNWs structurally resemble fibrous proteins in connective tissue and extracellular matrix (ECM), which are main cell adhesion substratum in vivo. Hemispherical silicon microbroccolis (SiMBs) possess large contact area with microscale topology for cell contact and attachment. Mouse 3T3 fibroblasts were cultured on microscale and nanoscale silicon structures with different surface modifications. Silicon scaffolds were functionalized by several physical and chemical vapor deposition methods to modify scaffold surface physical and chemical properties. Metal-coated SiNWs and SiMBs had been demonstrated and compared the ability to provide mechanical support sites for cell adhesion and promote cell proliferation and maintain normal cell functionality. Scanning electron microscope (SEM) micrographs at high magnification show cell-scaffold interactions, and immunofluorescence images reveal nuclear DNAs and actin cytoskeleton distribution on nanostructure covered substrates and selected biomarker expression was analyzed by enzyme-linked immunosorbent assay (ELISA).

1. Introduction

Tissue engineering is a promising technology combining engineering, science and human biology to approach and solve problems in human health. One of the major goals is to regenerate or restore functional tissues and organs in extracorporeal artificial systems for future graft implantation. Based on the design goal, the cell-substrate interaction is important for tissue engineering. Basement membrane is a structure that serves as substrata for overlying cell. Basement membranes consist of extracellular matrix (ECM) that contains fibrous and glycogen-attached protein frameworks as structural and connective components in a bulk tissue. The effects of surface science on cell adhesion, cell migration, cytoskeletal rearrangement, tissue response have been explored extensively in the past few decades. The mechanical properties, such as matrix rigidity, of materials also influence fundamental cell behaviors. In addition to biochemical and mechanical properties, the substratum topography, including both micrometer and nanometer scales, has direct effects on the abilities of cell to orient, migrate, and organize cytoskeletal arrangement. The previous studies used scanning electron, transmission electron microscopy, and atomic force microscopy to observe and measure the features and sizes of cell basement membrane.[1,2] They found that basement membranes are composed of a complex mixture of nanometric pores, ridges, and fibers. The report also showed that the nanostructured of silicon fibers exhibited highly a bactericidal activity and demonstrated that it's a novel antimicrobial nanomaterial in the field of mechano-microbiology[3]. On the other hand, the architectures of nano-surface could inference cell compatibility and bactericidal activity.

Filamentous nanomaterials, such as nanotubes[4], nanowires[5] and nanorods[6], are potential substituents for fibrous biomolecular scaffold in an artificial culture system. Carbon nanofibers (CNFs) with unique chemical, physical and electrical properties have been proved their feature in biomedical applications.[7] Owing to outstanding mechanical properties, scientists have successfully achieved the use of CNFs as scaffold in bone[8,9] and neural tissue engineering.[10,11] Bioengineers also applied semiconductor III-V compound nanofibers to neurons culture.[12] One-dimensional silicon nanomaterials are attractive building blocks for self-assembly nanoelectronic devices[13,14], and real-time biological nanosensors.[15,16] Several nanowire growth mechanisms have been developed, such as template-assisted synthesis[17], laser ablation[18], chemical vapor deposition (CVD)[19], electrochemical deposition[20], and vapor-liquid-solid (VLS).[21] Most of the recent successful semiconductor nanowire growth is based on the VLS technique. This crystal synthesis method is well known, and it could produce nanometric (nanoscaled) features with controlled dimensions and specific shapes.

[a] Department of Materials Science and Engineering, National Cheng Kung University, Tainan, Taiwan.
[b] National Nano Device Laboratories, Tainan, Taiwan.
[c] Institute of Oral Medicine, National Cheng Kung University, Tainan, Taiwan.
*E-mail: tmlee@mail.ncku.edu.tw; Fax: +886-6-2095845; Tel: +886-6-2387321
[d] School of Dentistry, Kaohsiung Medical University, Kaohsiung, Taiwan

To date, various topographical features such as grooves, ridges, stops, pores, nodes, islands in microscale have been used to cultures many kinds of cells. The majority of these studies employed photolithography to produce controlled, microscale, regular, repeating features for the cell behavior. These microscaled topographies can influence cellular initial attachment, migration, and differentiation. Some reports indicated that cells aligned to the long axis of the grooves, and the organization of actin and cytoskeletal elements also aligned along grooves.[22] Besides, nanoscaled topography has received increasing attention because cells interact with extracellular matrix components in nanometric scale. Several methods were used to create nanopatterened surface for cell culture substrate or cell-based sensors.[23] In our recent study[24], the nanoscaled topography of titanium alloy would influence the initial cell adhesion force by cytodetachment method. In this study, silicon nanowires (SiNWs) were synthesized by metal-catalyzed vapor-liquid-solid (VLS) method, and then surface treatment was further used to modify the surface chemistry of specimens. In addition to nanoscaled topography, microscaled topography was also achieved by metal-catalyzed VLS method. The aim of this experiment was to realize what factors of nanoscaled topography would influence 3T3 fibroblast behavior comparing with those of microscaled topography.

2. Materials and methods

2.1 Synthesis of silicon nanowires (SiNWs) and silicon microbroccolis (SiMBs)

In this study, bottom-up strategy was applied to synthesize silicon scaffold. Silicon substrates (1 cm x 1 cm) were cleaned by semiconductor RCA cleaning process to remove physically attached and chemically bonded contaminants on the surface. RCA cleaning process consists of serial dipping in SPM (H_2SO_4:H_2O_2=3:1, v/v), DHF (HF:H_2O=1:50, v/v), APM (NH_4OH:H_2O_2:H_2O=1:1:5, v/v) and CPM (HCl:H_2O_2:H_2O=1:1:6, v/v) for 600 s, 60 s, 600 s and 600 s, respectively. Nanoscale gold thin film was then sputtered onto substrates, and gold was essentially used as catalyst to initiate and accelerate synthesis. Sputtering was carried out by Hitachi E-1010. The deposition rate was 8 nm/min at controlled discharge current of 16-18 mA for 50 s. Gold-coated substrates were loaded into a low-pressure furnace with different SiH_4 supply for silicon scaffold synthesis, the reaction temperature was maintained at 620 ^oC. The experimental process flow is sketched in Fig. 1A. The diameter and size of silicon structure can be adjusted by different SiH_4 concentration supplied in the process. Nano-scale SiNWs were synthesized in the gas mixture SiH_4:N_2=1:4 for 20 min as shown in Fig. 1B,C. At low magnification (Fig. 1B), synthesized SiNWs show random growth orientation constructing adequate surface contact area for cell adhesion. The SEM image at magnification of 140,000 shows nano-roughness on the surface of SiNWs (Fig. 1C). The silicon structure synthesized in the 100% SiH_4 environment for 1 h has microscale diameter and length (Fig. 1D), and broccoli-like appearance, therefore, silicon microbroccolis (SiMBs) was used for this second silicon microstructure throughout the study.

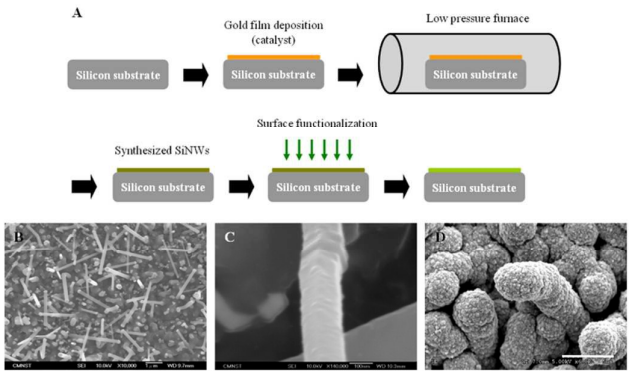

Figure 1. (A) Schematic demonstration of fabrication process flow. (B) SEM micrograph of SiNWs (20% SiH4 supplied in the synthesis) at high magnification (10,000 X). (C) Nano-scale surface roughness of SiNWs (140,000 X). (D) SEM micrograph (5,000 X) of SiMBs with larger diameter and compact configuration (100% SiH_4 supplied). The porosity and dimension of silicon structure are tunable in synthetic process to satisfy different spatial requirements for cell development.

2.2 Surface functionalization

We performed 5 different surface modifications: (1) oxidization, (2) nitrification, (3) gold coating, and (4) titanium coating. Oxidization and nitrification was performed using atmospheric pressure chemical vapor deposition (APCVD) and plasma-enhanced chemical vapor deposition (PECVD), respectively, and metal was coated by thermal evaporator. The thickness of materials deposited on silicon structures was 200 angstroms. Plus raw SiNWs, there were five experimental groups. After modification, structural integrity of scaffold remained consistent.

2.3 Cell culture

We utilized high-temperature and high-pressure process to sterilize silicon structure-covered substrates before cell seeding. Mouse 3T3 fibroblasts were culture in T-75 flasks filled with small amount of Dulbecco's Modified Eagle's Medium (DMEM) containing 10% bovine calf serum (GIBCO) and 1% Penicillin-Streptomycine-Amphotericin B solution (Cashmere Biotech) at precisely controlled temperature of 37 ^oC in a 5% CO_2 incubator. Cell number in the flask was enumerated and the volume was diluted with fresh medium to reduce cell number to suitable seeding number depending on the substrate area.

2.4 Cell Morphology

Fibroblasts were seeded (50,000 cells/cm^2) on nanostructure-covered substrates placed in a 24-well culture plate (TCP) for 30 min, 1 h, 3 h and 6 h incubation. Silicon substrates were removed from the plate as culture time stopped, immersed into a Petri dish filled with 2.5% glutaraldehyde and placed in a 4^oC refrigerator overnight to fix cells on the substrate. After fixation, substrates were washed in 5% phosphate buffered saline (PBS) and dipped in 1%

osmium tetroxide (OsO_4) solution for 1 h at room temperature. Next, substrates were rinsed in PBS several times to remove residual carcinogenic OsO_4 solution and incubated with 1% tannic acid for 1 h. The purpose of tannic acid immersion was to increase electron density on cell membrane for further SEM observation. Serial dehydration was performed by dipping substrates in 30%, 50%, 70%, 95% and 100% ethanol. The final step, all substrates were covered by hexamethyldisilazane (HMDS) in a Petri dish and air dried in a laminar-flow hood. Completely dehydrated substrates were coated with gold and observed by Hitachi scanning electron microscope (SEM) S-3000H.

2.5 MTT assay

The vitality of fibroblasts was analyzed by 3-(4,5-dimethyldiazol-2-yl)-2,5 diphenyl tetrazolium bromide (MTT) reduction assay. The assay measures the succinate dehydrogenase mitochondrial activity on the basis of colorimetry. Fibroblasts were cultured (50,000 cells/cm^2) on 5 experimental substrates and multi-well culture plate as control group for 1, 3 and 7 days. The medium was changed every 48 hours. 200 µL MTT solution was added into each well, and incubated for 4 h. Aspirated the solution, 1 mL DMSO was added into the wells, the plate was mildly shook to mix DMSO and purple color crystals at the bottom, incubated for 30 min. The absorbance was measured 562 nm wavelength using an ELISA reader.

2.6 Immunofluorescence imaging

Immunofluorescence staining was performed to visualize biomolecules distribution. Cell-attached substrates were washed in 5% PBS and immersed in 4% paraformaldehyde overnight. After fixation, substrates were serially added 0.1% non-ionic Triton X-100 for 5 min and 1% BSA for 30 min at room temperature. Monoclonal anti-actin antibodies (mAbs, 1:5000 dilution, Calbiochem) in 1% BSA was used against actin filaments (α-, β- and γ-isoforms) at room temperature for 1 h and red-fluorescent rhodamine-conjugated secondary antibodies (1:100 dilution, Calbiochem) in 1% BSA was introduced to recognize primary antibodies for 1 h at room temperature. Finally, we counterstained nuclear DNAs with DAPI (Sigma) for 1 h which is blue-fluorescent dye bound to DNA minor grooves to indicate locations of nuclei under confocal microscope. The emission wavelength of DAPI and rhodamine is around 461 nm and 570 nm, respectively. Well prepared substrates were observed by Olympus FV 1000 confocal laser scanning biological microscope.

2.7 ELISA assay

Cells (100,000 cells/cm^2) were seeded on Ti-coated SiNWs and 24-well TCP (control) for 6, 12 and 24 h. After incubation, cell lysis buffer was added in each well at room temperature for 5 min. In the lysis process, cell membrane was dissolved releasing cellular composition to medium. We collected lysate and medium in each well as sample solutions, then performed assay to analyze total fibronectin amount. Each 20 µL sample solution was injected into single wells of 96-well ELISA plate, after that, 80 µL coating buffer in ELISA Kit package (GenScript) was added into wells partly filled with sample solution in order to immobilize proteins on plate surface. After 20 min immobilization, buffer and floating biomolecules were removed by washing solution rinse. Rabbit-originated polyclonal anti-fibronectin antibodies (1:20 dilution, Abcam) were applied against anchored fibronectins. The primary antibody-antigen interaction took 30 min on a shaker to complete. Again, unconjugated antibodies and residual buffer were rinsed off. Enzyme-linked secondary antibodies were then introduced to specifically bind to primary antibody-antigen complexes at room temperature for 20 min. Rinse after sandwich-like antibody-antigen interaction was significant to reduce background noise. Substrates for linked enzymes, 3,3',5,5'-Tetramethylbenzidine (TMB), were added to produce visual signals for ELISA reader (Tecan, Sunrise). Fluorogenic substrates can be used instead for higher sensitivity and precision. After addition of stopping buffer, the blue reaction solution turned yellow. Absorbance of the converted dye was measured at a fixed emission wavelength of 452 nm.

2.8 Statistical analysis

Data was processed using ANOVA methods and verified by Duncan's multiple range test to obtain statistical significance. A $p<0.05$ was considered significant.

3. Results

3.1 SEM observation of cell morphology

As shown in Fig. 2, cell morphological changes on nanostructure were observed by SEM. As culture time prolonged, from 30 min to 6 h, fibroblasts on some modified SiNWs scaffolds maintained adhesion to homogeneous SiNWs substrates. Especially on gold- and titanium-coated SiNWs, cell morphology fast changed from round shape to well spread comparing with other substrates (Fig. 2A,B). As cells cultured in a multi-well plate, cell attaches smoothly and flatly to plate bottom is a reference identifying cell physiological and proliferation conditions. This result suggested that metal-coated silicon nanomaterials provide an environment for initial cell adhesion. Obvious SiNWs penetration through cell membrane can be seen (Fig. 2C), cell membrane completely engulfed SiNWs on contact sites. Cell membrane deformation and curvature was caused by serial dehydration and rinsing (Fig. 2C). SiNWs were tightly engulfed by cell membrane (Fig. 2D,E), and SiNWs at the edge of cell membrane were covered by unknown material (Fig. 2E) probably secreted by cell. Due to cell locomotion and hydrodynamic force generated by medium substitution and rinsing, membrane crack debris on SiNWs was shown (Fig. 2F). Ultrastructures appeared on nuclear protrusions cultured on Ti-coated SiNWs, less to be found on other SiNWs substrates (Fig. 2G). This ultrastructure is a possible result of cytoskeleton remodeling during the adhesion process.

Cytoplasmic prolongation (Fig. 2H,I) is a mechanical process of cell behavior generally including transformation in appearance, cytoskeleton reorganization underlying cell membrane, organelles and factors spacial redistribution in

cytoplasm. It is also a reference of cell physiological condition identification. Cell moves and homes to a specific location within a tissue, explores and responds to the environmental stimuli, physically contacts with surrounding cells, vigorous cytoplasmic prolongation is the most essential step. The same kinetics can be identified on osteoblasts cultured on carbon nanofiber scaffold.[25] The measured diameter of a single fibroblast on a pure silicon substrate was approximately 20 to 25 μm, diameter of fully spread cells on SiNWs ranged from 30 to 40 μm. The longest pseudopod-like cytoplasmic prolongation measured so far exceeded 78 μm. Metal-coated silicon scaffold is non-cytotoxic based on our experimental results and previous report.[26]

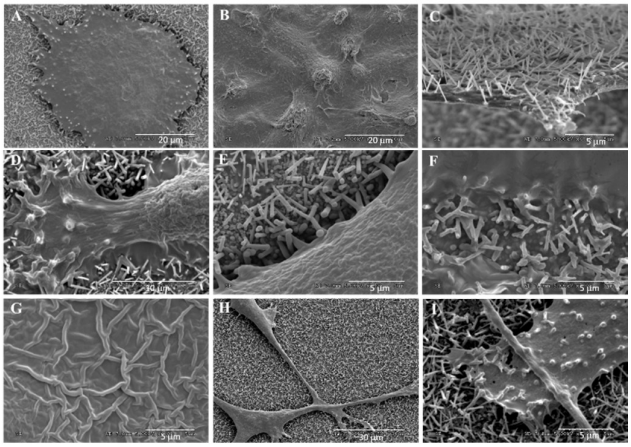

Figure 2. Morphological changes of fibroblasts grew on SiNWs. (A) Single cell well spread and adhesion to a Ti-SiNWs-covered substrate, the culture was 3 h. (B) Multiple-cell membrane fusion forming a network on Au-coated silicon nanostructure in 6 h, spherical knobs were nuclei. (C) SiNWs penetrated cell membrane (curvature caused by serial dehydration and rinsing). Cells were cultured on nitrified SiNWs for 3 h. (D) Close-up view of cell-Ti-SiNWs interaction within 1 h. Muscle–like furrow on extended cell membrane was induced by cytoskeleton reorganization beneath. (E) After 6h culture, obvious cell-Ti-SiNWs interaction at higher magnification. Note the SiNWs surface was covered by cell secreted material and membrane. (F) Cell membrane debris on Ti-SiNWs probably caused by cell movement and hydrodynamic force in medium. The culture time was 3 h. (G) Cultured on Ti-coated SiNWs for 3 h, repeated observation of ultrastructure on cell membrane, especially on nuclei protrusions. (H) Cytoplasmic prolongation was observed on Au-coated SiNWs after 3 h incubation . (I) Membrane fusion can be seen at cytoplasmic prolongations physical contact interface. The substrate was Au-SiNWs and the culture time was 3 h.

3.2 Cell proliferation on SiNWs

Data of MTT (Fig. 3) assay were statistically processed with significant $p<0.05$ (n>3) at 1, 3 and 7 days. In the 1-day culture, the OD values of oxidized, nitrified, Au-coated, and Ti-coated SiNWs was significantly higher than control group. This result indicated that the SiNWs structure could provide the environment for initial cell adhesion. It should be paid attention to that OD values of oxidized and nitrified SiNWs decreases from 1-day culture to 3-day. The Au-coated and Ti-coated SiNWs presented significantly higher OD value than control groups after 3-day culture. After 7-day culture, the decrease of OD value was observed for oxidized, nitrified, and Au-coated SiNWs. The Ti-coated SiNWs also showed statistically higher OD values than control groups at 7-day culture.

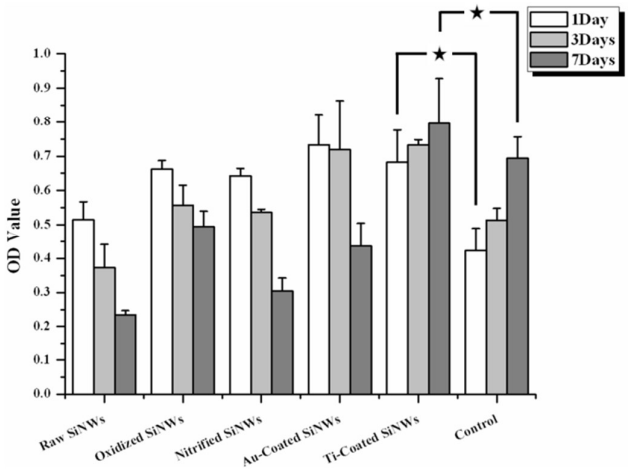

Figure 3. MTT assay result with standard deviation. Fibroblasts were seeded on SiNWs, oxidized SiNWs, nitrified SiNWs, Au-coated SiNWs, Ti-coated SiNWs and TCP (control), and cultured for 1, 3, and 7 days (n>3, *$p<0.05$).

3.3 Immunofluorescence imaging of cytoskeletal molecules

Cell-cell communication interface (Fig. 4A,B) was visualized at molecular level, white arrow in the figure points at cytoplasmic prolongations contact interface. Red filaments in the picture represent complex actin isoforms network. Actin filaments provided framework support for membrane outgrowths while succeeding soluble molecules exchange and organelles displacement took place within membrane fusion portion (Fig. 2H,I).

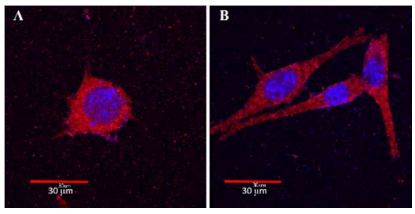

Figure 4. Immunofluorescence visualization of biomolecules on Ti-coated SiNWs for 6 h incubation. Blue spots (DAPI) show nuclear DNAs, red filaments (rhodamine) show F-actins. (A) White arrow indicates cell-cell communication interface. (B) Obvious cytoplasmic prolongation.

3.4. Structure size effect on cell proliferation and morphology

Structure size effect on cell response was another issue we tried to investigate. We supplied 100% SiH_4 in the synthetic process to construct SiNWs with higher planar density, thicker diameter (micrometer scale), higher surface roughness and

less porosity. SEM micrographs of fibroblasts incubated on second-type silicon microstructure, silicon microbroccolis (SiMBs), for 1 and 6 h was shown in Fig.5A-D. In the SEM micrograph (Fig. 5A), half cell body flatly adhered to SiMBs, note there was a pseudopod-like outgrowth (arrow) from half spherical body reached nearby structure. This micrograph shows cell's step-wise spread process. Cell scouts surroundings with sensitive outgrowths for suitable location to begin division and proliferation. Incubation for a longer time, large-area multi-cell network formed on the substrate (Fig. 5D).

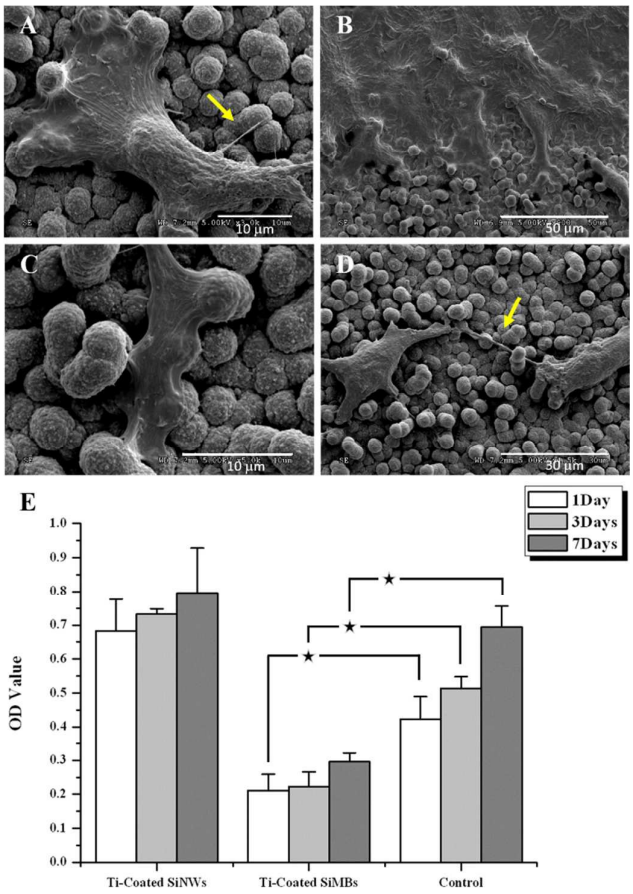

Figure 5. Morphological changes of fibroblasts grew on raw SiMBs substrates and MTT assay result with standard deviation (n>3). (A) 1 h cell culture. A pseudopod-like outgrowth (arrow) contacted nearby nanostructure before further spread. (B) 6 h cell culture. Multi-cell network formed on a substrate. (C) 1 h cell culture. Close-up view of cell-nanostructure interaction. (D) 1 h cell culture. Cytoplasmic outgrowth can be identified by arrow. (E) MTT assay result (n>3, **p*<0.05).

Growth on a SiMBs substrate, it was very difficult for a cell to completely engulf nanostructure it touched, cells became to envelop it instead (Fig. 5C). Cells manipulated physical envelopment to obtain required contact area for tight adhesion. Neurite-like cytoplasmic prolongation was again observed (Fig. 5D). Interestingly, cell proliferation on SiMBs expressed in similar trend but less cell proliferation than cells on SiNWs substrates (Fig. 5E). To simplify the statement of MTT result, statistical significance values were directly labeled on MTT diagram, all $p<0.05$.

3.5. Cell functionality examination

In order to investigate SiNWs-induced influence on cell functionality, immunofluorescence staining and ELISA were performed to analyze fibronectin (FN) distribution and expression. Biomolecules staining procedure was similar to previously stated protocol, monoclonal anti-fibronectin antibodies (1:1000 dilution, Calbiochem) and DAPI were used in the major staining step. Immunofluorescence imaging (Fig. 6) shows intracellular distribution of fibronectin and location of nucleus. The abundant fibronectins surrounding nucleus can be facilely identified, the area of expressed FN was almost equal to the area of cytoplasm. Subsequently, cellular fibronectin expression was analyzed by ELISA. ELISA can be classified as an immunological assay to quantitatively and qualitatively detect infinitesimal amount of specific antigen, or protein marker, expressed or secreted by a living organism. As shown in Figure 7, the OD values, represented the cellular fibronectin expression, of Ti-coated SiNWs increased with longer culture period.

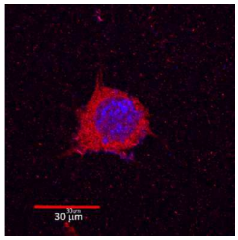

Figure 6. Visualization of fibronectin distribution within a single cell cultured on Ti-coated SiNWs for 6 h culture.

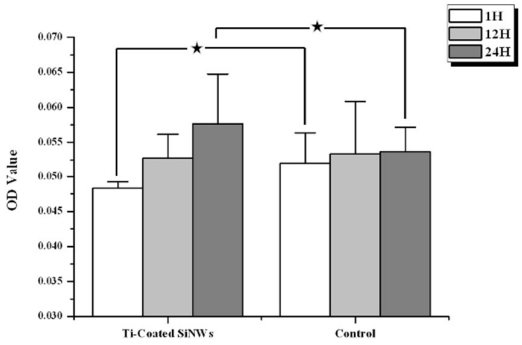

Figure 7. ELISA analysis of cellular fibronectin expression on Ti-coated SiNWs and TCP at three time points (n>3, **p*<0.05).

4. Discussion

Several investigations reported that cellular metabolism was in association with the surface topography, chemical composition, surface energy and surface charge of biomaterials.[27] It has been reported that microscaled topography would directly affect the ability of cells to orient themselves, migrate, and produce organized cytoskeletal arrangements. The extracellular matrix (ECM) is secreted by cells and surrounds them in tissues. The basement membrane

is the thin layer of ECM that provides mechanical structure and modulates cell behavior. The mechanical properties of basement membrane influence fundamental cell behaviors. The strained collagen matrix would induce fibroblast to produce more tenascin and collagen XII than relaxed matrix.[28] Basement membranes possess a complex, three-dimensional topography consisting of nanometer sized features. A number of microfabrication techniques, such as soft lithography, photolithography, plasma polymerization, laser ablation, grit-blasting, etching, were used to manufacture the microscaled and nanoscaled topography for implant, tissue engineering, cell-based sensors and drug discovery.[29,30] Recently, nanowire prepared by VLS method is at the early stage of biological application. In VLS mechanism, the nanowires grow with the aid of a catalytic metal particle. Gaseous reactants supersaturate a catalytic liquid located on a solid substrate, and the liquid-solid interface becomes the nucleation site for a single crystal structure. Hallstrom have used VLS method to deposit vertical gallium phosphide (GaP) nanowire on substrate.[11] *In vitro*, the never cells interacted closely with the nanostructures, and cell survival was better on nanowire substrates than on planar control substrates. Kim et al cultured mammalian cells on vertically aligned silicon nanowires array substrates.[31] The nanowires could physically penetrate the cells and deliver gene into cells. In this study, VLS method was used to deposit fibrous, random, and mesh structure on substrates. The mesh-like SiNWs is designed to mimic the extracellular matrix, and surface modification is used to improve the biocompatibility for cell responses.

The effect of nanoscale fibrous structure on cell responses was tested with five kinds of surface composition. By observation of SEM (Fig. 2), the cells appear to flatten, spread, and take on the morphology of the underlying respective specimens. The SEM images suggest that the cell morphology is mainly influenced by the nanoscale structure rather than surface chemistries in this study. At higher magnification, the fibrous structure of SiNWs allows them to penetrate cells or to be engulfed by cells on contact sites. The results suggest that SiNWs could provide the topography for cell initial adhesion at the early stage. The initial interactions occurring at the tissue-implant interface largely determine the success or failure of an implant. Surface texture, a combination of topography and roughness, has been found to directly effect on the attachment of cells and their subsequent proliferation and differentiation. Osteoblast, for example, has been shown to be sensitive to surface roughness and exhibit greater initial attachment to rough titanium surface.[32]

In the present study, it was found that after culture period of 1 day the cell number was higher on five types of SiNWs than control group. Increased cell number, indicated by the higher optical density, on SiNWs could be attributed to that cell might easily attach to rough and fibrous structure. The early phenomenon (during 1 day) apparently did not influence further proliferation. As shown in Fig. 3, a decrease in cell number as a function of time was observed in as-deposited, oxidized and nitrified SiNWs throughout the 1-7 day culture periods, and Au-coated SiNWs showed the significant lower cell number at 7-day culture than 3-day culture. Apparently, the increases in cell number were found for Ti-coated SiNWs from 1 to 7 days. The major differences in surface composition could affect cell proliferation. Titanium is a cyto-compatible metal widely used as raw or coating material in medical instruments and implants. In oral and orthopaedic application, the results show that implants made of or coated with titanium have good interaction and fuse easily with osteoblasts, in vivo bone-forming cells.[33] This property significantly reduces immunological rejection and promotes cure rate of clinical treatments.

Among five kinds of SiNWs, Ti-SiNWs show the best cytocompatibility and the potential application for further study. It means different chemistry properties in SiNWs could affect cell behavior. However, there is still one question that the cell behavior on Ti-SiNWs is influenced by nanoscale structure or composition. The effect of microscale and nanoscale topography on fibroblast cell responses was tested with same surface composition. As shown in Fig. 2A and 5A, cells spread well on Ti-SiNWs substrates than Ti-SiMBs. On the same surface composition substrates, after 1 day, cell adhesion was significantly improved and approximately 3.5 times more cells to the Ti-SiNWs substrate than Ti-SiMBs (Fig. 5). After 7-day culture, cell number is still approximately 2.8-fold on Ti-SiNWs compared to Ti-SiMBs. Based on cell morphology and proliferation, this implies that nanoscale structure with Ti coating plays an important role in cell responses.

Fibroblasts are in vivo stroma-forming cell maintaining tissue structural integrity and commonly used as feeder for specific cell lines, such as keratinocytes and stem cells, in vitro. Proliferation rate of fibroblasts is significant, therefore, this cell line is a desirable biological model for cytotoxicity and biocompatibility examination of scaffold material. Latest research indicated that using nuclear transplantation technique to deliver important gene fragments into fibroblasts can reprogram them to an induced pluripotent state as certain stem cells.[34] These outstanding results emphasized the importance of fibroblasts in future regenerative medicine research. In a living organism, fibroblast secrets ECM essential proteins into adjacent tissue and circulatory system, which provides high-concentration fibronectin (FN) to be utilized by other cells working on tissue structure maintenance, wound healing, development and differentiation regulation. Fibronectin is a widely distributed plasma glycoprotein dimmer with approximate molecular weight of 250 kDa, it exists in ECM and cell surface in a complex multimeric form. In vivo expression of FN is also an indicator to be analyzed for tumor uncontrollable proliferation and subsequent metastasis. Futhermore, we selected Ti-coated SiNWs for ELISA analysis based on their significant proliferation enhancement. ELISA diagram (Fig. 7) shows consistent increase in fibronectin (FN) amount using Ti-coated SiNWs substrate along incubation time. In Fig. 7, the increasing slope of OD values of total FN expression collected from lysate and medium on Ti-coated SiNWs is more obvious than the control. The FN expression of cells cultured on TCP almost maintained at the same amount

as incubation time increased. This result can be interpreted that cells stably proliferate and demonstrate modified functionality on Ti-coated SiNWs scaffold.

The advantages of using SiNWs as cell growth scaffold can be classified as following points. First, SiNWs are highly integrable to bio-microsystems in many levels, for example, MEMS-compatible synthesis process and synthesis area can be defined by photolithography process. Second, the growth density can be perfectly controlled to construct an ECM mesh-like microenvironment as a tool to study cell mechanotransduction, a mechanism involves in cell behavior, adhesion, migration, proliferation and differentiation regulation via external mechanical stimuli. In vivo, tissue and ECM are soft, therefore, protein or polymer immobilization onto rigid SiNWs substrate is a strategy to functionalize a softer surface for cell adhesion. Finally, bio-molecules immobilization onto silicon surface is easy through chemical treatment to make surface hydrophobic-hydrophilic property alteration and deposition or coating adhesion layer for proteins. The biocompatibility of silicon nanostructures for in vivo animal research should be tested in the future work.

5. Conclusions

The aim of the study was to construct a silicon-based microenvironment for cell adhesion and growth and evaluate the cyto-compatibility of microscale and nanoscale scaffold with different functionalizations. We analyzed the effect of modified silicon microstructure and nanostructure as planar scaffold on fibroblast proliferation and functionality in this work. Assay results show the scaffold functionalization with titanium can generate remarkable influences on cell proliferation and selected biomarker expression which is considered as an indicator of cell physiological condition growing on the silicon scaffold. On the contrary, raw, oxidized, nitrified and gold-coated SiNWs show anti-proliferation effect. Structurally compared, collagen fibril-like Ti-SiNWs performed better than microscale Ti-SiMBs on the basis of proliferation assay result. This outcome suggests that synthesized nanowires, nanocylinders, nanorods which dimensionally resemble fibrous structural proteins in connective tissue and basal lamina are potential building blocks for artificial microenvironment as tools for cell biology research. The study provides a new strategy using non-biological functionalization of scaffold promoting cell vitality in tissue engineering. The surface chemical and physical properties that efficiently promote cell adhesion and stimulate proliferation is the principal topic in the future investigation.

Acknowledgements

This study is supported by Ministry of Science and Technology (AZ-10-09-30-104) and Kaohsiung Medical University (KMU-KMUH Co-Project of Key Research, grant No. KMU-DK105005).

References

1 E. Martínez, E. Engel, J.A. Planell, J. Samitier, *Annals of Anatomy - Anatomischer Anzeiger*, 2009, **191**, 126-135.
2 V. Raghunathan, C. McKee, W. Cheung, R. Naik, P.F. Nealey, P. Russell,. *Tissue Eng. Part A*, 2013, **19**, 1713-1722.
3 E. P. Ivanova, J. Hasan, H. K. Webb, G. Gervinskas, S. Juodkazis, V. K. Truong, A. H. F.Wu, R. N. Lamb, V. A. Baulin, G. S. Watson, J. A. Watson, D. E. Mainwaring, R. J. Crawford,. *Nat. Commun.,* 2013**, *4***, 2838.
4 T. Rafeeqi, G. Kaul, *J. Biomed. Nanotechnol.*, 2010, **6**, 710-717.
5 B. Tian, J. Liu, T. Dvir, J. Jin, J.H. Tsui, Q. Qing. *Nat. Mater.*, 2012, **11**, 986-94.
6 Y. Ogawa, M.S. White, L. Sun, M.C. Scharber, N.S. Sariciftci, T. Yoshida, *Chemphyschem*, 2014, **15**, 1070-75.
7 W. Lee, V. Parpura, Chapter 6 - Carbon nanotubes as substrates/scaffolds for neural cell growth. *Prog. Brain. Res*, 2009, **180**, 110-25.
8 Y. Wan, G. Zuo, F. Yu, Y. Huang, K. Ren, H. Luo, *Surf Coat Technol*, 2011, **205**, 2938-2946.
9 R. Vasita, D.S. Katti, *Int J Nanomedicine*, 2006, **1**, 15-30.
10 M.C. Chuang, H.Y. Lai, J.A. Ho, Y.Y. Chen, *Biosens Bioelectron*, 2013, **41**, 602-607.
11 W. Hallstrom, T. Martensson, C. Prinz, P. Gustavsson, L. Montelius, L. Samuelsonl. *Nano Lett*, 2007, **7**, 2960-2905.
12 J.W. Thomas, C.W. Michael, L.M. Janice, L.P. Rachel, U.E. Jeremiah, *Nanotechnol*, 2004, **15**, 48-54.
13 Y. Wu, Y. Cui, L. Huynh, C.J. Barrelet, D.C. Bell DC, C.M. Lieber, *Nano Lett*, 2004, **4**, 433-436.
14 L.J. Chen, *J Mater Chem*, 2007, **17**, 4639-4643.
15 G. Zheng, C.M. Lieber, *Methods Mol Biol*, 2011, **790**, 223-237.
16 M.O. Noor, U.J. Krull, *Anal Chim Acta*, 2014, **825**, 1-25.
17 Z. Chen, Y. Li, J. Jiang, C. Cao, T. Xu, Q. Chen, *RSC Adv*, 2012, **2**, 6806-6809.
18 M. Hasan, M.F. Huq, Z.H. Mahmood, *Springerplus*, 2013, **2**, 151.
19 H. Suzuki, H. Araki, M. Tosa, T. Noda, *Mater Trans*, 2007, **48**, 2202-2206.
20 L. Liu, *Sci China Technol Sci*, 2005, **58**, 362-368.
21 H.J. Yang, F.W. Yuan, H.Y. Tuan, *Chem Commun*, 2010, **46**, 6105-6107.
22 M. Nikkhah, F. Edalat, S. Manoucheri, A. Khademhosseini, *Biomaterials*, 2012, **33**, 5230-5246.
23 H. Jeon, C.G. Simon, G. Kim, *J Biomed Mater Res B Appl Biomater*, 2014, **102**, 1580-1594.
24 C.C. Wang, Y.C. Hsu, F.C. Su, S.C. Lu, T.M. Lee, *J Biomed Mater Res A*, 2009, **88**, 370-387.
25 L.P. Zanello, B. Zhao, H. Hu, R.C. Haddon, *Nano Lett*, 2006, **6**, 562-567.
26 N. Sachot, O. Castaño, M.A. Mateos-Timoneda, E. Engel, J.A. Planell, *J R Soc Interface*, 2013, **10**, 20130684.
27 Biomaterials science : an introduction to materials in medicine. In: Ratner BD, editor. 2nd ed. ed. Amsterdam ; Elsevier Academic Press; 2004.

28 M. Chiquet, M. Matthisson, M. Koch, M. Tannheimer, R. Chiquet-Ehrismann, *Biochem Cell Biol*, 1996, **74**, 737-744.
29 M. Ni, W.H. Tong, D. Choudhury, N.A.A. Rahim, C. Iliescu, H. Yu, *Int J Mol Sci*, 2009, **10**, 5411-5441.
30 C.J. Bettinger, R. Langer, J.T. Borenstein, *Angew Chem Int Ed Engl*, 2009, **48**, 5406-5415.
31 W. Kim, J.K. Ng, M.E. Kunitake, B.R. Conklin, O. Yang, *J Am Chem Soc*, 2007, **129**, 7228-7229.
32 B.D. Boyan, C.H. Lohmann, D.D. Dean, V.L. Sylvia, D.L. Cochran, Z. Schwartz, *Annu Rev Mater Res,* 2001, **31**, 357-371.
33 T.J. Webster, J.U. Ejiofor, *Biomaterials*, 2004, **25**, 4731-4739.
34 M. Wernig, A. Meissner, R. Foreman, T. Brambrink, M. Ku, K. Hochedlinger, *Nature*, 2007, **448**, 318-324.

Graphic abstract